

M.S. THESIS

# Reinforcement learning of cellular networks for glucose homeostasis

혈당 항상성을 유지하는 세포 네트워크에 대한 강화학습

BY

JAEWOOK JEONG

FEBURARY 2024

DEPARTMENT OF PHYSICS EDUCATION  
COLLEGE OF EDUCATION  
SEOUL NATIONAL UNIVERSITY

M.S. THESIS

# Reinforcement learning of cellular networks for glucose homeostasis

혈당 항상성을 유지하는 세포 네트워크에 대한 강화학습

BY

JAEWOOK JEONG

FEBURARY 2024

DEPARTMENT OF PHYSICS EDUCATION  
COLLEGE OF EDUCATION  
SEOUL NATIONAL UNIVERSITY

# Reinforcement learning of cellular networks for glucose homeostasis

혈당 항상성을 유지하는 세포 네트워크에 대한 강화학습

지도교수 조 정 호

이 논문을 석사 학위논문으로 제출함

2024년 2월

서울대학교 대학원

물리교육과

정 재 욱

정재욱의 석사 학위 논문을 인준함

2024년 2월

위 원 장:	채승철	(인)
부위원장:	석효준	(인)
위 원:	조정호	(인)

# Abstract

The islets of Langerhans, composed of alpha, beta, and delta cells, are essential for regulating glucose homeostasis via hormonal regulation. This study presents a novel method for analyzing the regulatory mechanisms of these cells by leveraging reinforcement learning within a simulated islet environment, inspired by prior research. We conceptualized this scenario as a multi-agent multi-armed bandit (MAMAB) problem and employed the Upper Confidence Bound (UCB) approach to examine cellular interaction dynamics.

Our research was carried out in two primary phases: the first assessed the effect of various glucose conditions on the stability and flexibility of cellular interactions. The second phase investigated the influence of different islet counts on these interactions and the overall stability of the system. Findings indicate that specific interactions consistently support glycemic balance and adapt well to changes in external glucose levels, both in hyperglycemic and hypoglycemic states, independent of islet quantity.

This study significantly contributes by merging data on hormone secretion and glucose fluctuations into a unified numerical scoring framework, offering a comprehensive assessment of cellular interactions. It reveals the underlying mechanisms of effective intercellular communication within islet environments across diverse scenarios and suggests that exploring natural islet cell interactions through reinforcement learning provides insights into their evolutionary and functional aspects.

**keywords:** Glucose Homeostasis, Islets of Langerhans, Reinforcement Learning, Multi-Agent Multi-Armed Bandit (MAMAB), Cellular Interactions

**student number:** 2022-25506

# Contents

<b>Abstract</b>	<b>i</b>
<b>Contents</b>	<b>ii</b>
<b>List of Tables</b>	<b>iv</b>
<b>List of Figures</b>	<b>vi</b>
<b>1 Introduction</b>	<b>1</b>
<b>2 Background</b>	<b>3</b>
2.1 Dynamics and Interactions of Pancreatic Islet Cells . . . . .	3
2.2 Concepts of Reinforcement Learning . . . . .	9
<b>3 Experiment and Results</b>	<b>17</b>
3.1 Experimental Setup . . . . .	17
3.2 Experimental Procedure and Methodology . . . . .	20
3.3 Results and Analysis . . . . .	23
3.3.1 Optimal interaction with external blood glucose levels . . . . .	23
3.3.2 The impact of the number of islets . . . . .	29
<b>4 Conclusion</b>	<b>34</b>
<b>Appendix A Top Reward Table by Interaction Type</b>	<b>40</b>

<b>Appendix B Optimal Interactions Relative to the Reward Coefficient</b>	<b>42</b>
<b>Appendix C Experimental results of optimal interaction based on the number of islets</b>	<b>45</b>
<b>Abstract (In Korean)</b>	<b>47</b>

# List of Tables

2.1	Observed interaction signs of islet cells . . . . .	4
3.1	Cumulative reward over 50 timesteps as a function of islet number in normoglycemic conditions without interactions. . . . .	30
A.1	Top reward table in normal glucose settings . . . . .	41
A.2	Top reward table in high glucose settings . . . . .	41
A.3	Top reward table in low glucose settings . . . . .	41
A.4	Top reward table in non-stationary glucose settings . . . . .	41
B.1	Top-5 frequent interaction table at $\rho = 2$ in stationary glucose settings	43
B.2	Top-5 frequent interaction table at $\rho = 5$ in stationary glucose settings	43
B.3	Top-5 frequent interaction table at $\rho = 10$ in stationary glucose settings	43
B.4	Top-5 frequent interaction table at $\rho = 0.5$ in stationary glucose settings	44
B.5	Top-5 frequent interaction table at $\rho = 0.2$ in stationary glucose settings	44
B.6	Top-5 frequent interaction table at $\rho = 0.1$ in stationary glucose settings	44
C.1	Top-5 optimal interactions at islet number $N = 1$ . . . . .	45
C.2	Top-5 optimal interactions at islet number $N = 5$ . . . . .	45
C.3	Top-5 optimal interactions at islet number $N = 10$ . . . . .	46
C.4	Top-5 optimal interactions at islet number $N = 50$ . . . . .	46
C.5	Top-5 optimal interactions at islet number $N = 100$ . . . . .	46

C.6	Top-5 optimal interactions at islet number $N = 200$ . . . . .	46
-----	--	----



# List of Figures

2.1	Natural interaction signs of islet cells. Red triangle arrow means activation and blue bar arrow means inhibition. . . . .	4
2.2	Robust islet cell networks. . . . .	8
2.3	Variations in hormone secretion over time by interaction type. The graph illustrates that hormone secretion is more pronounced in scenarios without interaction (dotted orange line) as opposed to instances of natural type interaction (solid blue line). . . . .	10
2.4	Fluctuations in glucose levels over time by interaction type. This figure demonstrates that the absence of interaction (dotted orange line) leads to greater fluctuations in glucose levels as opposed to the natural type of interaction (solid blue line), which also shows a gradual increase over time. . . . .	10
3.1	Top-5 most frequent interaction figure in normal glucose condition and abnormal glucose condition experiments. . . . .	25
3.2	Top-5 most frequent interaction figure in high glucose condition and low glucose condition experiments. . . . .	26
3.3	Temporal dynamics of hormone secretion and glucose levels by interaction type. The left side of the figure represents the dynamics under normal glucose conditions, while the right side depicts the corresponding changes in an abnormal glucose environment. . . . .	27

3.4	Temporal dynamics of hormone secretion and glucose levels by Interaction type in varied glucose conditions. For the high glucose condition, shown on the left, the figures demonstrate the response patterns in an elevated glucose environment. Conversely, the right side of the figure focuses on the low glucose condition. . . . .	28
3.5	Hormone secretion and glucose level by islet number in the absence of interaction. Generally the higher the islet number, the more stable the hormone secretion and the glucose level. . . . .	31
3.6	Hormone secretion and glucose level by islet number in the nature interaction, at high glucose. Generally the higher the islet number, the more stable the hormone secretion and the glucose level. . . . .	32
3.7	Optimal interactions and their percentages in high blood sugar (top) and low blood sugar (bottom) when the number of islets was 200. The natural interactions were first in high blood sugar and second in low blood sugar. . . . .	33

# Chapter 1

## Introduction

Blood glucose, or blood sugar, is critical for cellular energy, making its homeostasis essential for metabolic functioning. Disturbances in this equilibrium can precipitate serious conditions like diabetes. The pancreas contains specialized endocrine tissues, the islets of Langerhans, which play a central role in regulating blood glucose homeostasis. These islets are predominantly composed of  $\alpha$ ,  $\beta$ , and  $\delta$  cells, accounting for over 90% of the islet cell population. Each cell type is integral to the hormonal regulation of blood glucose, facilitating complex interactions that either stimulate or inhibit hormone secretion [1]–[3].

Prior studies [4], [5] have significantly contributed to our understanding of cellular interactions within the islets of Langerhans, focusing on the hormonal outputs of alpha, beta, and delta cells. These investigations explored the dynamics of these cells within a single islet, considering both the internal cellular interactions and the feedback between the islet and its external environment. Specifically, these models have been pivotal in elucidating how a triad of one  $\alpha$ , one  $\beta$ , and one  $\delta$  cell functions in tandem, responding to and influencing their surrounding milieu.

The insights gleaned from these studies have been crucial in identifying interactions that effectively maintain both hormone secretion levels and blood glucose homeostasis. However, it's important to note that these models, while comprehensive, have

their limitations. They conceptualize hormone secretion and glucose fluctuations as independent variables and utilize a somewhat simplified model for external glucose input. Moreover, these frameworks have yet to fully explain why certain cellular interactions, commonly observed in natural islet environments, are more prevalent over other theoretically favorable interactions.

To overcome these challenges, we have integrated reinforcement learning into our research. This approach, reminiscent of genetic algorithms, involves an agent learning optimal behavior through rewards in a specific environment, potentially illuminating the evolutionary trajectory of islet cell interactions [6]–[8].

In this paper, we develop a multi-agent reinforcement learning environment with islet cells as agents. We designed a reward system based on the amalgamation of hormone secretion and blood glucose fluctuation, focusing on the interaction types between cells. We framed this as a multi-agent multi-armed bandit problem and applied the Upper Confidence Bound (UCB) algorithm in a context similar to independent Q Learning, aiming to identify robust interactions under various conditions. Our results highlight the significant stability of natural islet interactions, especially under high glucose conditions, and demonstrate that stability in hormonal interactions occurs when cells engage in anti-symmetric interaction types.

The paper is structured as follows: Chapter 2 introduces the biophysical model of islet cells from prior studies, along with the concept and algorithm of reinforcement learning used in our research. Chapter 3 details the experimental environment and discusses the results of the experiments, and Chapter 4 concludes the paper.

## Chapter 2

### Background

#### 2.1 Dynamics and Interactions of Pancreatic Islet Cells

The islets of Langerhans, a specialized cluster of cells in the pancreas, consist of various cell types, primarily including  $\alpha$ ,  $\beta$ ,  $\delta$ ,  $\epsilon$ , and PP cells. The  $\alpha$ ,  $\beta$ , and  $\delta$  cells, which constitute the majority of these islets, play a crucial role in the regulation of blood glucose levels through hormonal secretion [9], [10].

$\alpha$  and  $\beta$  cells collaborate to balance blood glucose in the body.  $\alpha$  cells produce glucagon, which elevates blood glucose levels, whereas  $\beta$  cells secrete insulin to reduce them.  $\delta$  cells, secreting somatostatin, modulate the hormonal activities of both  $\alpha$  and  $\beta$  cells. This intricate network of hormone secretion and interaction is vital in maintaining glucose homeostasis [11], [12].

The hormones glucagon, insulin, and somatostatin, secreted by  $\alpha$ ,  $\beta$ , and  $\delta$  cells respectively, not only regulate blood glucose levels but also influence each other's secretion. Glucagon encourages hormone release from *beta* and *delta* cells, while insulin suppresses secretion from  $\alpha$  cells and promotes it in  $\delta$  cells. Conversely, somatostatin acts as an inhibitor for both  $\alpha$  and  $\beta$  cells. These complex interactions are schematically depicted in Table 2.1 and Figure 2.1.

From cell $\rightarrow$ to cell	Interaction type	Sign
$\alpha \rightarrow \beta$	activation	+
$\alpha \rightarrow \delta$	activation	+
$\beta \rightarrow \alpha$	inhibition	-
$\beta \rightarrow \delta$	activation	+
$\delta \rightarrow \alpha$	inhibition	-
$\delta \rightarrow \alpha$	inhibition	-

Table 2.1: Observed interaction signs of islet cells

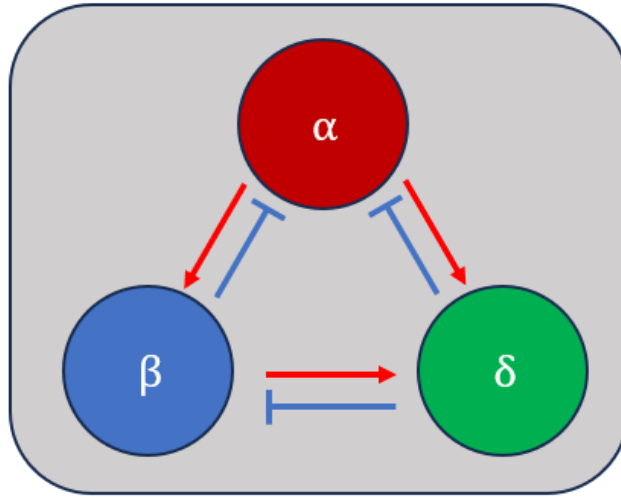


Figure 2.1: Natural interaction signs of islet cells. Red triangle arrow means activation and blue bar arrow means inhibition.

## Modeling Blood Glucose Dynamics

The variation in blood glucose levels, influenced by glucagon  $H_\alpha$  from  $\alpha$  cells and insulin  $H_\beta$  from  $\beta$  cells, is captured by the following equation (2.1) [4], [5] :

$$\frac{dG}{dt} = \lambda(G_0 \cdot H_\alpha - G \cdot H_\beta) + G_{\text{ext}}(t). \quad (2.1)$$

Here,  $\lambda$  is a coefficient representing the impact of hormones on blood glucose levels, measured in units of  $\text{min}^{-1}$ .  $G_0$  denotes the basal blood glucose level, approximately 4mM, and  $G$  is the current blood glucose level.  $G_{\text{ext}}(t)$  signifies external glucose input.

## Hormonal Secretion Dynamics

Each cell type, represented by  $\sigma \in \{\alpha, \beta, \delta\}$ , secretes hormones based on its phase  $\theta_\sigma$  and amplitude  $r_\sigma$ , described by equation (2.2):

$$H_\sigma = r_\sigma \cdot \frac{1 + \cos \theta_\sigma}{2}. \quad (2.2)$$

Next two steps, we will further explore the time-dependent variations of  $\theta_\sigma$  and  $r_\sigma$ .

## Phase Modulation in Islet Cells

The phase modulation is a dynamic process with the phase  $\theta_\sigma$  oscillating between 0 and  $2\pi$ . This modulation is mathematically expressed in equation (2.3) [4], [5] :

$$\frac{d\theta_\sigma}{dt} = \omega_\sigma + g_\sigma(G) \cdot \cos \theta_\sigma + \kappa \sum_{\sigma' \neq \sigma} A_{\sigma\sigma'} \cdot \frac{r_{\sigma'}}{r_\sigma} \cdot \sin(\theta_{\sigma'} - \theta_\sigma), \quad (2.3)$$

where  $\omega_\sigma$  indicates the intrinsic phase period of each cell type, typically around  $2\pi/5$  minutes. The term  $g_\sigma(G)$  is a cell-specific phase modulation factor, which varies depending on the current blood glucose level  $G$ . The modulation factor for each cell type

is detailed in equations (2.4 - 2.6):

$$g_\alpha(G) = \mu \cdot (G - G_0), \quad (2.4)$$

$$g_\beta(G) = -\mu \cdot (G - G_0), \quad (2.5)$$

$$g_\delta(G) = -\mu \cdot (G - G_0). \quad (2.6)$$

Here,  $\mu$  signifies the phase modulation's impact on the phase change, measured in units of  $0.5 \text{ min}^{-1} \text{ mM}^{-1}$ . This model ensures that in high glucose conditions ( $G > G_0$ ), alpha cells spend more time in a low-hormone-secreting phase ( $[\pi/2, 3\pi/2]$ ), while beta and delta cells rapidly exit this phase.

The final term in equation (2.3) accounts for phase changes resulting from cellular interactions.  $\kappa$ , set at  $1 \text{ min}^{-1}$ , determines the interaction effect's magnitude. The interaction term  $A_{\sigma\sigma'}$  is an integer that can take values of -1, 0, or 1, representing the type of interaction between cells  $\sigma'$  and  $\sigma$ , where -1 indicates inhibition, 0 denotes no interaction, and 1 signifies secretion.

### Amplitude Modulation in Islet Cells

Amplitude modulation is a dynamic process influenced by the current blood glucose level. This modulation is governed by equation (2.7) [4], [5] :

$$\frac{dr_\sigma}{dt} = (f_\sigma(G) - r_\sigma^2) \cdot r_\sigma + \kappa \sum_{\sigma' \neq \sigma} A_{\sigma\sigma'} \cdot r_{\sigma'} \cdot \cos(\theta_{\sigma'} - \theta_\sigma), \quad (2.7)$$

where  $f_\sigma(G)$  represents the amplitude modulation factor, unique to each cell type and dependent on the blood glucose level  $G$ . The specific modulation factor for each cell



type is detailed in Eqs. (2.8 - 2.10):

$$f_{\alpha}(G) = \frac{1}{2} \cdot \left[ 1 - \tanh \left( \frac{G - G_0}{\eta} \right) \right], \quad (2.8)$$

$$f_{\beta}(G) = \frac{1}{2} \cdot \left[ 1 + \tanh \left( \frac{G - G_0}{\eta} \right) \right], \quad (2.9)$$

$$f_{\delta}(G) = \frac{a_{\delta}}{2} \cdot \left[ 1 + \tanh \left( \frac{G - G_0 + G_{\delta}}{\eta} \right) \right]. \quad (2.10)$$

In this model,  $\eta$ , approximately 5mM, modulates the amplitude response relative to the deviation of blood glucose  $G$  from the baseline  $G_0 = 4$  mM. The condition  $0 < a_{\delta} < 1$  implies that insulin secretion by beta cells surpasses somatostatin secretion by delta cells. Additionally,  $G_{\delta}$ , about 2mM, indicates a heightened sensitivity of delta cells to glucose levels compared to other cells. According to Eqs. (2.7 - 2.10), the model is configured such that high blood glucose conditions lead to a decrease in the amplitude of alpha cells, subsequently reducing their hormone secretion as outlined in Eq. (2.2).

The influence of cellular interactions on amplitude modulation is represented by the last term in Eq. (2.7). This term underscores the interconnected nature of the islet cell network, where each cell type's activity impacts the others.

### Homeostasis Regulation in Islet Cells

The comprehensive model, encapsulated in Eqs. (2.1 - 2.10), demonstrates how the islet system maintains glucose homeostasis. In states of elevated blood glucose ( $G > G_0$ ), the system adapts by increasing insulin secretion and reducing glucagon output, thereby lowering glucose levels. Conversely, in low glucose conditions ( $G < G_0$ ), it responds by enhancing glucagon secretion and decreasing insulin production, which elevates the glucose levels.

## Modeling Blood Glucose Changes Across Multiple Islets

In previous research, the modeling of blood glucose changes was extended to include scenarios involving multiple islets functioning independently. This broader perspective is represented in the modified equation (2.11) [5]:

$$\frac{dG}{dt} = \frac{\lambda}{N} \left[ \sum_{k=1}^N (G_0 \cdot H_{\alpha_k} - G \cdot H_{\beta_k}) \right] + G_{\text{ext}}(t), \quad (2.11)$$

where  $N$  denotes the total number of islets. In this equation, the hormone secretion from each cell within an islet is summed and then averaged across the number of islets  $N$ . This approach effectively captures the cumulative impact of multiple islets on blood glucose dynamics, ensuring that the model remains stable and accurate even as the number of islets varies.

The focus of these studies was on identifying interactions that minimized hormone secretion and reduced fluctuations during blood glucose stabilization. The investigations covered both normal and high glucose conditions, including scenarios with continuous external glucose input, to determine robust interaction patterns. These findings are illustrated in Figure 2.2

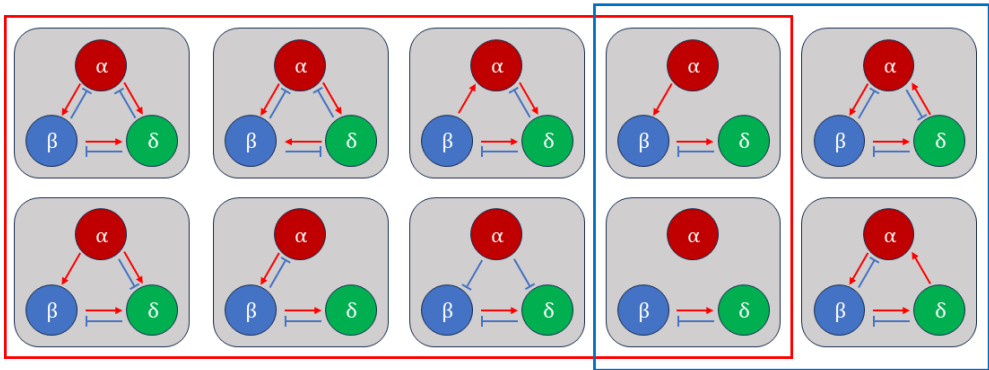


Figure 2.2: Robust islet cell networks.

In Figure 2.2, the top-left section depicts the natural interactions observed within the islets, with subset interactions highlighted in red squares. The top-right section

shows a variant of these natural interactions, operating in a similar manner but in a different asymmetric direction. The interactions deemed robust within this variant are marked in blue squares, representing a specific subset of the overall interaction pattern.

To elucidate the distinctions in cellular interactions, particularly in terms of hormone secretion and glucose fluctuation, a comparative analysis was conducted. Figures 2.3 and 2.4 offer graphical representations of these dynamics. They contrast scenarios with natural type cell interactions against those with no cell interaction, focusing on hormone secretion and glucose fluctuation over time.

In cases where there is no interaction between cells, each cell secretes hormones solely in response to glucose, governed by its current phase and amplitude. This situation results in less optimal outcomes both in terms of hormone regulation and glucose stability. Conversely, the natural interaction scenarios depicted in these figures demonstrate more effective regulation, highlighting the importance of cellular interplay in maintaining homeostasis.

## 2.2 Concepts of Reinforcement Learning

Reinforcement Learning (RL) emerges within machine learning as a distinctive method where agents refine their decision-making by actively interacting with an environment. Unlike supervised learning, which hinges on pre-labeled datasets, RL relies on an agent's capability to formulate strategies based on the rewards or penalties received from its actions. This approach diverges fundamentally from unsupervised learning, which is oriented towards identifying patterns in data without the influence of reward feedback. A central aspect of RL is its focus on the maximization of cumulative rewards over time, a feature that sets it apart from other learning methodologies [13], [14].

At the heart of RL is the interaction between the agent and the environment. In this setup, an agent is defined as an entity capable of making decisions or executing

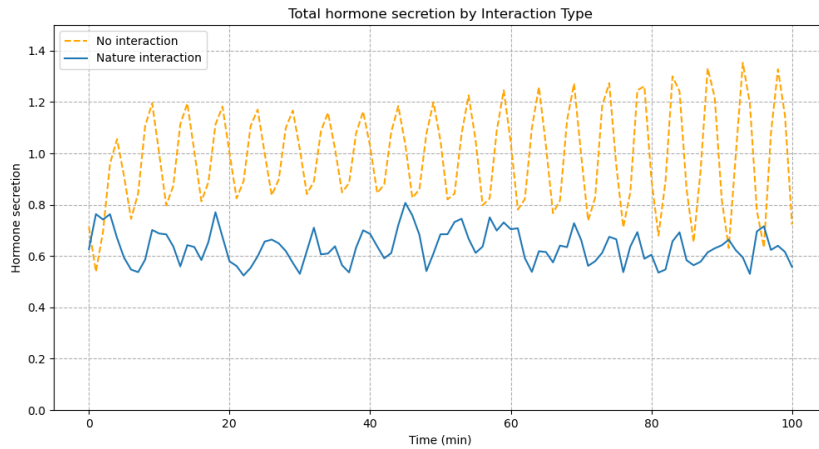


Figure 2.3: Variations in hormone secretion over time by interaction type. The graph illustrates that hormone secretion is more pronounced in scenarios without interaction (dotted orange line) as opposed to instances of natural type interaction (solid blue line).

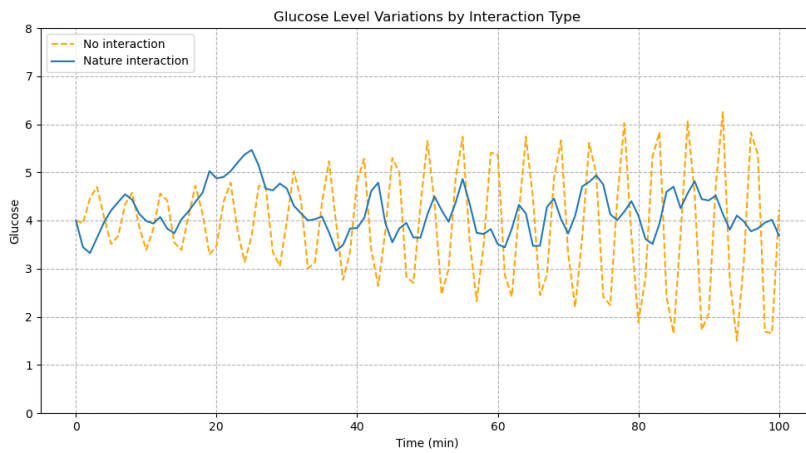


Figure 2.4: Fluctuations in glucose levels over time by interaction type. This figure demonstrates that the absence of interaction (dotted orange line) leads to greater fluctuations in glucose levels as opposed to the natural type of interaction (solid blue line), which also shows a gradual increase over time.

actions within an environment. This environment is typically modeled as a dynamic system, presenting a variety of scenarios or states for the agent to navigate. During each timestep, the agent assesses the current state of the environment, selecting an action from a range of available options. The environment responds to this chosen action by transitioning to a new state and allocating a corresponding reward or penalty. This reward serves as a measure of the action's effectiveness in achieving the agent's goals. The agent leverages the sequence of states, actions, and rewards to learn and refine its policy, a strategy dictating its actions in diverse states. The ultimate aim of the agent is to devise a policy that optimizes cumulative rewards, thereby mastering the most effective methods of environmental interaction. The dynamic and reciprocal relationship between the agent's decisions and the environmental responses is the fundamental mechanism of learning in RL.

The structure of Markov Decision Processes (MDP) is commonly employed in RL. An MDP is characterized by the tuple  $(S, A, P, R)$ , where  $S$  represents a set of states,  $A$  encapsulates a set of actions,  $P$  denotes the state transition probability matrix, and  $R$  signifies the reward function. Within this framework,  $P(s'|s, a)$  determines the likelihood of transitioning to a new state  $s'$  from the current state  $s$  following an action  $a$ , while  $R(s, a)$  quantifies the expected reward for that action. The primary goal in MDPs is to identify a policy  $\pi : S \rightarrow A$  that maximizes expected cumulative rewards. The Markov property, asserting that future states depend solely on the present state and action and not on prior sequences, simplifies the decision-making process. This principle is pivotal in RL, as it diminishes the complexity of problems, rendering MDPs a potent framework for an array of RL scenarios.

### **Multi-Armed Bandit Problem**

The Multi-Armed Bandit (MAB) problem is a cornerstone of Reinforcement Learning (RL), providing a framework for decision-making under uncertainty. It involves an agent faced with several choices, each associated with a distinct and unknown reward

distribution. The agent's objective is to maximize the cumulative reward over a series of selections. This task requires a strategic balance between exploring to ascertain the reward potential of each option (exploration) and exploiting known options to garner maximum rewards (exploitation) [13]–[16].

The rationale for employing the Multi-Armed Bandit (MAB) model in our study, particularly in the context of blood glucose regulation, is fundamentally tied to its capacity to render the state as static. This attribute is crucial when dealing with dynamic systems like those in biological contexts, where states such as current glucose levels or hormone secretions are constantly changing. If these states were to dictate the actions in a reinforcement learning model, it would result in actions that vary continuously with the state, leading to a lack of convergence and potentially biologically unrealistic outcomes.

In traditional reinforcement learning models, the variability in state often requires the agent's actions to adapt correspondingly, which could lead to a constantly shifting strategy that does not necessarily align with how biological systems operate. Biological processes tend to exhibit consistent patterns of response rather than constantly changing behaviors in reaction to every slight fluctuation in state variables. The MAB approach, by assuming a fixed state, circumvents this issue. It allows for the development of a stable action-selection strategy that is not overly sensitive to the fluctuations in state variables like blood glucose levels.

This fixed-state model is particularly advantageous in biological contexts. In our study of blood glucose regulation, for instance, the MAB model enables us to simulate how different types of cells within the islets of Langerhans might consistently respond to changes in glucose levels, without the complexity of their actions changing with every minor fluctuation in these levels. This approach not only ensures the convergence of actions across all states but also aligns more closely with biological realism, where cellular responses, while influenced by external conditions, do not vary drastically with every minute change in those conditions.

Moreover, the MAB model's emphasis on the action-selection process, independent of state fluctuations, offers a more streamlined and focused approach to understanding and modeling the decision-making processes in dynamic systems. This feature of MAB models makes them particularly suited for applications in healthcare and biological research, where rapid and consistent decision-making is essential.

In the MAB framework, at each timestep, the agent assesses the expected reward, or action value  $q_t(a_i)$ , for each action  $a_i$ . The goal is to estimate the action value as close as possible to the true value  $q_*(a_i)$ , defined by the expected reward for selecting action  $a_i$ :

$$q_*(a_i) \doteq \mathbb{E}[R_t | A_t = a_i], \quad (2.12)$$

where  $R_t$  is the reward obtained at time  $t$  for choosing action  $a_i$ . Effective strategies to balance exploration and exploitation, such as the epsilon-greedy algorithm, the Upper Confidence Bound (UCB), and Thompson sampling, are employed to enhance the decision-making process [17]–[19].

The Multi-Agent Multi-Armed Bandit (MAMAB) problem extends the MAB framework to scenarios involving multiple agents. Each agent independently selects from a range of options, with the reward distributions potentially varying among agents and being influenced by the collective set of actions. The reward in MAMAB is given by:

$$R_t = \text{Bandit}(A_t^1 = a_{i_1}^1, A_t^2 = a_{i_2}^2, \dots, A_t^N = a_{i_N}^N), \quad (2.13)$$

where  $A_t^j$  is the action chosen by the  $j$ th agent at time  $t$ . This multi-agent extension introduces greater complexity compared to single-agent scenarios, necessitating consideration of inter-agent interactions and collective strategy formation [8], [20]–[22].

MAMAB is particularly advantageous in environments where the actions of multiple decision-makers simultaneously impact the outcome. This model is relevant in situations where agents must not only learn from their individual experiences but also

adapt to the actions of others, a context that aligns well with scenarios like islet cell interactions in glucose regulation.

The complexity of the MAMAB model lies in its incorporation of multiple agents, each making decisions that impact not only their outcomes but also the outcomes of other agents in the environment. This interplay creates a rich tapestry of interactions, where the collective behavior significantly influences the dynamics of the system. In medical or biological contexts, such as the regulation of blood glucose by islet cells, understanding these interactions is crucial. Each agent (cell) not only responds to the external environment (blood glucose levels) but also to the actions of other cells, making the MAMAB model highly applicable.

In practical terms, MAMAB allows for the simulation of scenarios where the actions of one agent (or cell type) can have cascading effects on others. For instance, the secretion of insulin by beta cells not only lowers blood glucose levels but also affects the behavior of  $\alpha$  and  $\delta$  cells. In MAMAB, this is represented by the reward function, which takes into account the collective outcomes of these intertwined actions.

The application of MAMAB in modeling the interactions of islet cells offers several advantages. Firstly, it provides a framework to study how cells might optimally react not just to the blood glucose level, but also to the actions of other cells. Secondly, it allows for the exploration of various strategies that cells might employ in different glucose scenarios, contributing to a deeper understanding of the underlying mechanisms of glucose regulation. Finally, the MAMAB model, with its focus on multi-agent interaction and reward optimization, offers a powerful tool for predicting and analyzing the outcomes of different regulatory strategies, which can be invaluable in designing treatments for conditions like diabetes.

Moreover, the MAMAB framework aligns with the stochastic nature of biological systems, where outcomes are not always deterministic but influenced by a range of variables. By modeling these variables and their interactions, MAMAB provides insights into the probabilistic behavior of biological systems, offering a more nuanced



understanding than models which consider only single-agent scenarios or deterministic outcomes.

Therefore, the MAMAB model extends the principles of MAB to more complex, multi-agent environments, making it a versatile tool for exploring the dynamics of systems where multiple agents interact and influence each other. This is particularly relevant in biological systems, where multiple entities (such as cells, enzymes, or neurotransmitters) interact in complex ways to regulate various physiological processes.

### Upper Confidence Bound Strategy

The Upper Confidence Bound (UCB) strategy plays a critical role in resolving the exploration-exploitation trade-off inherent in Multi-Armed Bandit (MAB) problems. This strategy is particularly advantageous in scenarios where a balance is required between exploring new actions and exploiting known rewarding ones. UCB is designed to systematically manage the uncertainty associated with the estimation of action values, thereby guiding the decision-making process in a more informed manner.

UCB operates by adjusting the selection of actions based on both the estimated rewards and the uncertainty or variance associated with these estimates. The decision rule for selecting an action at time  $t$ , denoted as  $A_t$ , is given by:

$$A_t = \arg \max_{a_i} \left[ q_t(a_i) + c \sqrt{\frac{\ln t}{\text{Num}_t(a_i)}} \right], \quad (2.14)$$

where  $q_t(a_i)$  is the current estimated value of action  $a_i$ ,  $c$  is a tunable parameter that balances exploration and exploitation,  $\ln t$  represents the natural logarithm of the timestep  $t$ , and  $\text{Num}_t(a_i)$  is the number of times action  $a_i$  has been selected up until time  $t$ .

The first term,  $q_t(a_i)$ , represents the exploitation component, guiding the agent to select actions that have historically yielded high rewards. The second term,  $c \sqrt{\frac{\ln t}{\text{Num}_t(a_i)}}$ , accounts for exploration, encouraging the agent to try actions that have been selected

less frequently. The constant  $c$  controls the degree of exploration; a higher value of  $c$  promotes exploring less-known actions, while a lower value encourages sticking with actions that are already known to be rewarding.

In the context of our study, the Upper Confidence Bound (UCB) algorithm is especially advantageous for modeling environments like islet cell interactions, where the reward distribution can be considered relatively stationary or subject to slow changes over time. UCB adeptly negotiates the balance between exploration (trying out new actions) and exploitation (leveraging known rewarding actions), a critical aspect in environments characterized by uncertainty and variability. Unlike strategies such as epsilon-greedy, which rely on arbitrary exploration rates, UCB incorporates a systematic approach to determine the extent of exploration necessary at each step.

This feature of the UCB algorithm is particularly relevant in the context of our research on blood glucose regulation. The ability of UCB to make well-informed decisions without the need for arbitrary exploration parameters aligns well with the complexities of biological systems, where each decision could have significant implications. The algorithm's efficiency in balancing exploration and exploitation makes it a suitable choice for this study, ensuring that the model remains both robust and adaptable in the face of varying biological conditions. This balance is essential in ensuring that the learning process is both efficient and robust, particularly in situations where the cost of exploration is high, or the opportunities for learning are limited. In such scenario, the UCB algorithm's methodical approach to decision-making can lead to more effective and reliable outcomes [16], [23].

## **Chapter 3**

### **Experiment and Results**

#### **3.1 Experimental Setup**

In our study focusing on the complex interactions within the islets of Langerhans, the adoption of Reinforcement Learning (RL) is driven by its adaptability and efficiency in dealing with dynamic biological systems. Unlike static reward calculation methods, RL is exceptionally capable of adjusting to the ever-changing nature of biological environments. This adaptability is crucial in accurately modeling the nuanced interactions of islet cells, where variables and conditions are constantly in flux. RL's iterative learning process allows the model to accommodate and respond to these changes, providing a more realistic and effective representation of biological processes.

Another significant advantage of RL lies in its ability to uncover optimal strategies that may not be immediately apparent. Biological systems often present a vast array of interaction possibilities, many of which might be overlooked in a computation-based approach. RL, through its exploration and exploitation strategies, can navigate this complexity and reveal effective interaction patterns. This exploratory aspect of RL is particularly valuable in biological contexts, where the most effective strategies might not be intuitively obvious.

RL also aligns well with real-time decision-making requirements. Unlike static models that require constant recalculations with new data, RL can make decisions based on current information, making it well-suited for applications that demand timely responses. This feature is particularly relevant in the dynamic environment of islet cells, where conditions can change rapidly.

Lastly, the inherent variability and stochastic nature of biological systems are well-handled by RL. Traditional deterministic models might struggle with the unpredictable nature of biological processes. In contrast, RL's design accommodates a range of outcomes, learning from variability and uncertainty, which is a fundamental characteristic of biological systems.

In summary, RL's dynamic adaptability, exploratory capabilities, suitability for real-time decision-making, and ability to handle stochastic environments make it an ideal approach for our study. These attributes enable RL to model the complex cellular interactions within the islets of Langerhans more effectively than traditional computational methods, providing deeper insights into the mechanisms of glucose regulation.

### **Implementing the Islets of Langerhans Interaction as MAMAB**

Building on the foundational concepts discussed in the background section, our experimental investigation of islet cell interactions within the pancreas was conducted using the Multi-Agent Multi-Armed Bandit (MAMAB) framework. The decision to utilize MAMAB was driven by its ability to facilitate stable and consistent action selection, independent of the dynamic states of hormone secretion or blood glucose levels. This aspect of MAMAB is particularly beneficial in our study, as it aligns with the biological reality where cellular responses within the islets are not excessively variable despite fluctuations in their environment.

In contrast to traditional reinforcement learning methods, such as the Q-learning algorithm, which adapt actions in response to state changes, the MAMAB framework offers a strategic advantage. It allows for the evaluation and selection of actions based

on their effectiveness over time, rather than their immediate response to changing conditions. This ensures that the model remains focused on understanding and optimizing the long-term strategies of cellular interactions within the islets, a key factor in maintaining glucose homeostasis. Through this approach, our study aims to provide insights into the collective behavior of islet cells under different physiological scenarios, contributing to a deeper understanding of their role in glucose regulation.

## Experimental Configuration and Parameter Adjustments

Our experimental setup mirrors the original study’s framework, with modifications to certain parameters for clarity in interaction effects. Specifically, in equations (3-7) we set  $\mu = 0.1$  and  $\kappa = 0.4$ . These adjustments aim to enhance the visibility of interaction effects while moderating the intrinsic impact of cells on blood glucose levels outside the homeostatic range.

Furthermore, we modeled each type of cell within the islets of Langerhans —  $\alpha$ -cells,  $\beta$ -cells, and  $\delta$ -cells — as agents capable of performing 9 discrete actions. This approach is based on the understanding that each cell type can engage in one of three possible interaction types with the others. Considering two cells, this leads to  $3^2 = 9$  possible actions. To streamline our model, we utilized 20 islets, with the phase and amplitude of cells in each islet uniformly randomized within the ranges  $[0, 2\pi]$  and  $[0, 1]$ , respectively. In this setup, actions are uniform across all islets, meaning that identical cell types in different islets execute the same interactions. This standardization reduces the complexity of the exploration space for joint actions and provides a biologically realistic scenario.

The reward function  $r_t$ , applied to all agents at each timestep, is defined by Equation (3.1):

$$r_t = - \left( \left| \frac{dG}{dt} \right| + \rho \cdot \frac{1}{N} \sum_i^N \sum_{\sigma} H_{\sigma_i} \right), \quad (3.1)$$

This reward structure is designed to penalize both the rate of blood glucose change and the total hormone secretion by the islets. The goal is to minimize hormone output and glucose level oscillations, with the coefficient  $\rho > 0$  playing a crucial role in balancing the impact of glucose fluctuations and hormone levels. By default,  $\rho$  is set to 1, ensuring an equal emphasis on both factors. Consequently, agents are encouraged to collectively select actions that are in line with this reward strategy.

Using equation (3.1), Appendix A provides a detailed view of the five interactions yielding the highest rewards across different glucose states: normoglycemia, hyperglycemia, hypoglycemia, and abnormally dynamic glucose. This comprehensive compilation facilitates a deeper understanding of the most effective interaction types in various glucose conditions as determined by our Multi-Agent Multi-Armed Bandit (MAMAB) model.

## 3.2 Experimental Procedure and Methodology

### Episode Configuration and Learning Dynamics

Our experimental framework is structured around episodes, each consisting of 100 timesteps, mirroring a real-time duration of 100 minutes. At the conclusion of each episode, while the environment is reset to its initial state, the learned action values for each agent are preserved. This design choice facilitates the accumulation of learning across episodes, promoting the convergence of agent actions based on their experiences throughout the entire experimental sequence.

The comprehensive experiment spans 100 episodes, cumulatively covering 10,000 timesteps (minutes), thus providing a substantial period for observing learning dynamics and action convergence. To seed the learning process with variability, we initialize the action value for each possible action of an agent,  $q_t(a_i)$ , using values drawn from a Gaussian distribution characterized by a mean of 0 and a variance of 1.

Following the completion of this extensive series of experiments, our analysis fo-

cuses on identifying patterns in the agents' convergence towards specific sets of actions. By examining the data, we quantify the occurrence rates of these action sets, presenting our findings as percentages that reflect the prevalence of each converged action set throughout the experimental trials.

## Experimental Conditions

Our experimental framework was structured to assess the interactions within the islets of Langerhans under various glucose conditions. We employed two primary experimental paradigms to investigate these interactions.

The first set of experiments focused on evaluating optimal cellular interactions under different blood glucose levels: normal glucose, high glucose, low glucose, and non-stationary glucose. During the normoglycemia condition experiments, the starting blood glucose level was set at  $G_{\text{init}} = 4$  mM, reflecting the body's typical basal glucose level, and no external glucose was introduced or extracted. This setup allowed us to observe the islets' intrinsic regulatory mechanisms without external influences.

In the abnormal glucose condition experiments, we aimed to simulate variable glucose conditions. Here, the initial blood glucose level was set at  $G_{\text{init}} = 4$  mM, while the external glucose input  $G_{\text{ext}}$  was randomly selected between  $(-4, 4)$  mM every minute, following a uniform distribution. This approach was designed to test the islets' response to unpredictable and fluctuating glucose levels, further challenging their regulatory capabilities.

To maintain specific glucose conditions against the islets' homeostatic attempts to normalize blood glucose, while also ensuring the realism of blood sugar levels, we strategically manipulated external glucose inputs. In the high glucose experiments, we initiated the procedure with an initial blood glucose level of  $G_{\text{init}} = 8$  mM. To sustain a hyperglycemic state that mirrors realistic pathological conditions, we injected an additional  $G_{\text{ext}} = 4$  mM of glucose every minute. This approach was carefully calibrated to achieve elevated glucose levels without exceeding physiological plausibility.

Conversely, in the low glucose experiments, the starting glucose level was set at  $G_{\text{init}} = 2$  mM. To maintain a hypoglycemic state that aligns with realistically low but non-zero glucose concentrations, we extracted  $G_{\text{ext}} = -1$  mM every minute. This measured extraction rate ensured a gradual decrease in blood glucose levels, mirroring realistic scenarios of hypoglycemia.

These adjustments of external glucose inputs were crucial not only to counteract the islets' regulatory mechanisms but also to maintain blood sugar levels within ranges that are typically observed in clinical settings. By striking a balance between experimental rigor and physiological realism, our study aimed to closely simulate the conditions under which islet cells operate in the human body. This methodology enabled us to gain insights into the islets' behavior under various glucose states that are both experimentally controlled and realistically grounded.

In the second phase of our experimental study, we delved into analyzing the effects of varying numbers of islets on hormone secretion and blood glucose levels, with a particular focus on identifying the optimal interaction under these changing conditions. This experiment was designed to provide insights into the relationship between the number of islets and the efficacy of their collective interactions, a crucial aspect for understanding islet cell dynamics in diverse physiological states.

We methodically explored how the cumulative reward fluctuated when applying identical interactions across a constant glucose condition while varying the quantity of islets. This approach enabled us to assess the impact of islet count on the overall effectiveness of specific cellular interactions. By conducting this analysis, we aimed to discern patterns and trends in hormone secretion and blood glucose regulation that correlate with the number of islets present.

A pivotal part of this experiment involved the utilization of reinforcement learning techniques to ascertain the most effective or 'optimal' interaction type, especially in scenarios where the number of islets was significantly high. This analysis was crucial in understanding whether the interactions that emerged as optimal in a large islet ( $N =$



200) environment mirrored those observed in our first experiment, where  $N = 20$ . By comparing these outcomes, we sought to determine the consistency of optimal interactions across different scales of islet populations.

### 3.3 Results and Analysis

#### 3.3.1 Optimal interaction with external blood glucose levels

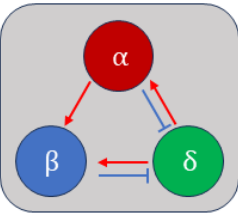
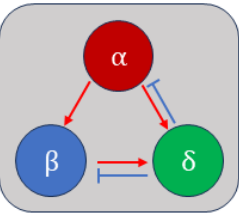
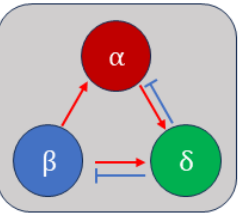
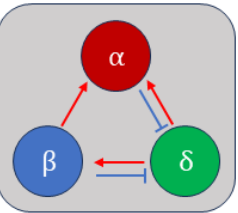
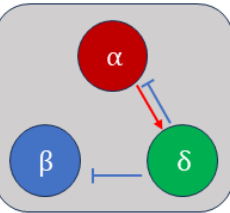
The experimental findings present a cohesive pattern across all conditions: the convergence of interactions predominantly belonged to Type 1. These outcomes are detailed in Figures 3.1 and 3.2, which depict the frequency of specific interaction types under various glucose states. Notably, in high glucose (hyperglycemic) conditions, the interaction type observed in nature was most prevalent, accounting for 34% of occurrences. Similarly, in low glucose (hypoglycemic) conditions, this natural interaction type was observed with the second-highest frequency, also at 34%. This indicates that natural interactions within islets are adept at managing rapid blood glucose fluctuations, such as those induced by eating or exercise, particularly in hyperglycemic or hypoglycemic scenarios. Conversely, under normal or dynamically changing glucose conditions, we observed a shift to interaction types different from those seen in nature.

Another critical observation is the absence of interactions that didn't fall into Types 1 and 2, suggesting that interactions where two cells either promote or inhibit each other's hormone secretion are not efficient for minimizing hormone secretion and maintaining glucose homeostasis. Figures 3.3 and 3.4 illustrate the variations in hormone secretion and glucose levels under different interaction types in each glucose condition. In all cases, either the interaction observed in nature or the most frequently occurring interaction proved more favorable than the absence of interaction, particularly regarding hormone secretion and blood glucose stability. Despite the no-interaction scenario appearing advantageous based on the average blood glucose values in high and low glucose states, this is misleading. The sharp oscillations in blood

glucose levels, as shown in the graphs, are a result of phase differences and high amplitude in the cells. Additionally, in high and low glucose conditions, the maintained high or low glucose levels under optimal or natural interactions are due to the external modulation of glucose. Once this external influence is removed, blood glucose levels promptly revert to normal, whereas in the no-interaction scenario, glucose levels do return to average but continue to exhibit significant oscillations.

In summary, these findings underscore that natural islet interactions are more effective in swiftly re-establishing steady-state blood glucose levels, especially when external factors induce rapid glucose changes. This insight highlights the efficiency of naturally occurring interactions within islets in responding to and managing dynamic glucose environments.

Additionally, we detail the experimental outcomes based on variations in  $\rho$  within Appendix B, examining how the significance attributed to hormone secretion and blood glucose fluctuations influences interaction patterns.

Top 5 most frequent interactions in normoglycemia condition					
Interaction					
Percentage (%)	20	14	12	9	7
Type	1	1	1	1	1

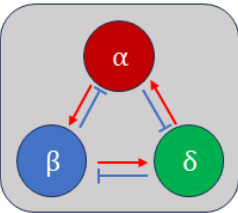
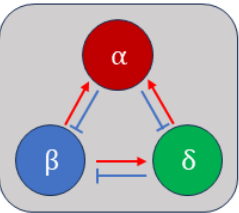
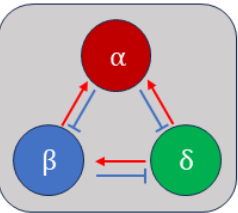
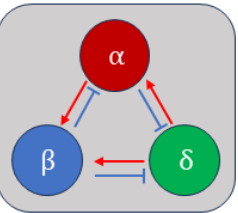
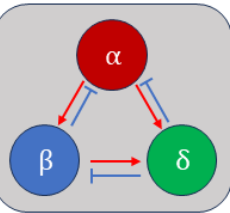
Top 5 most frequent interactions in abnormal glucose condition					
Interaction					
Percentage (%)	13	11	9	8	7
Type	2	1	1	1	1

Figure 3.1: Top-5 most frequent interaction figure in normal glucose condition and abnormal glucose condition experiments.

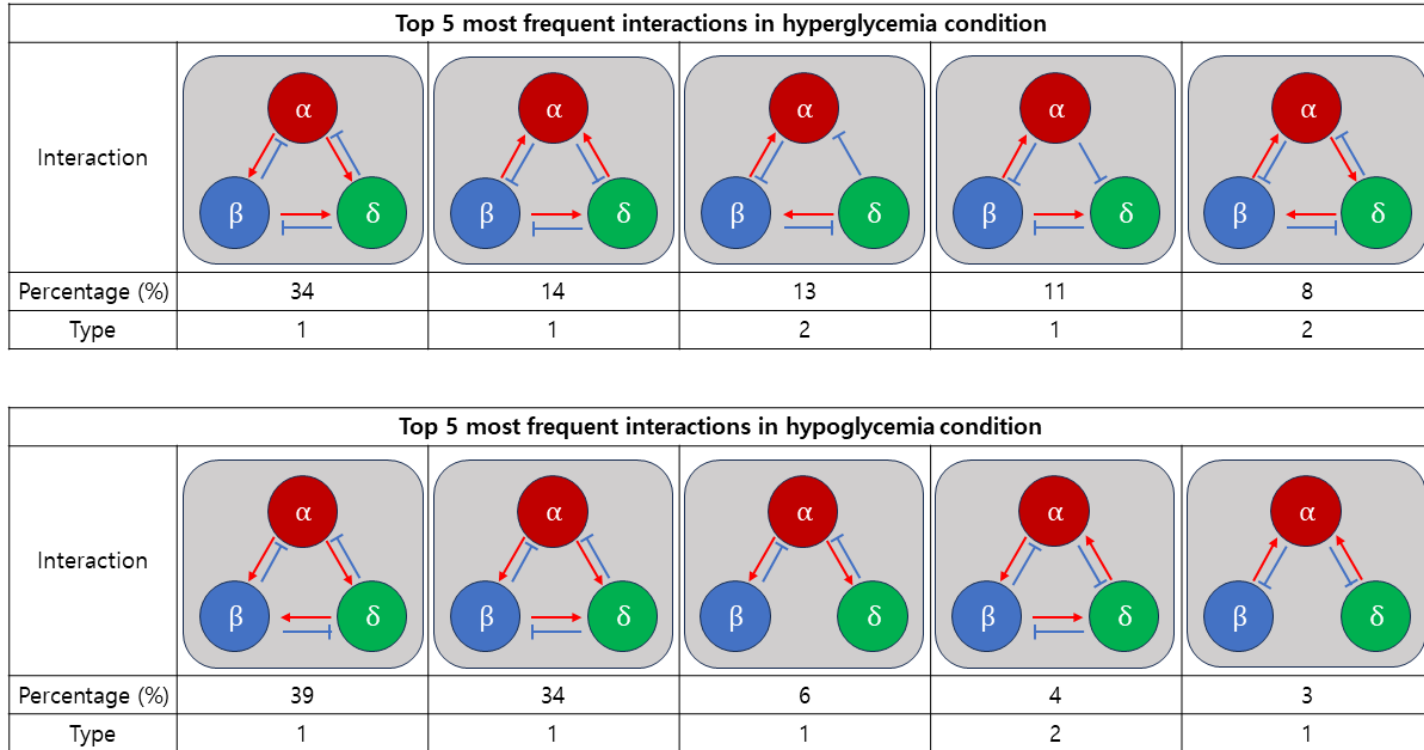


Figure 3.2: Top-5 most frequent interaction figure in high glucose condition and low glucose condition experiments.

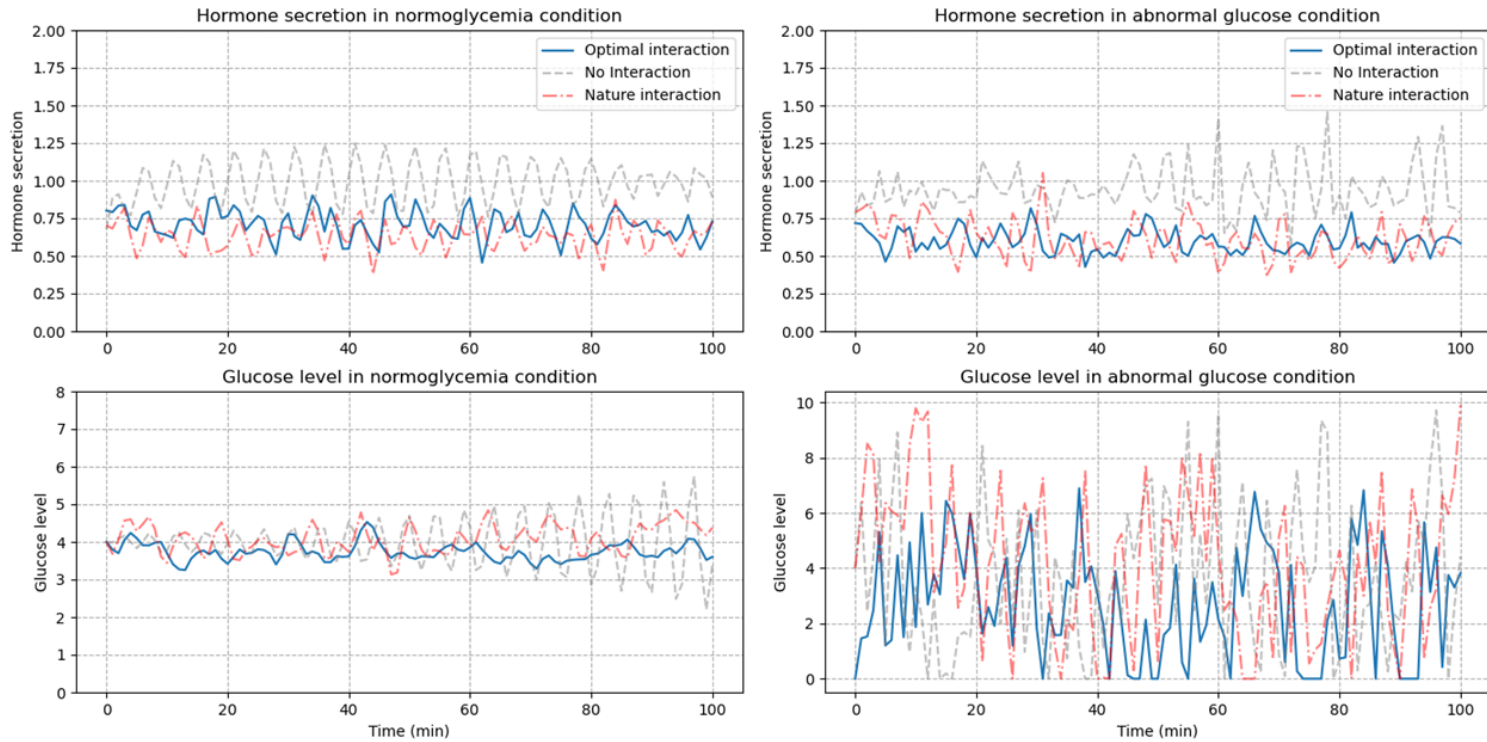


Figure 3.3: Temporal dynamics of hormone secretion and glucose levels by interaction type. The left side of the figure represents the dynamics under normal glucose conditions, while the right side depicts the corresponding changes in an abnormal glucose environment.

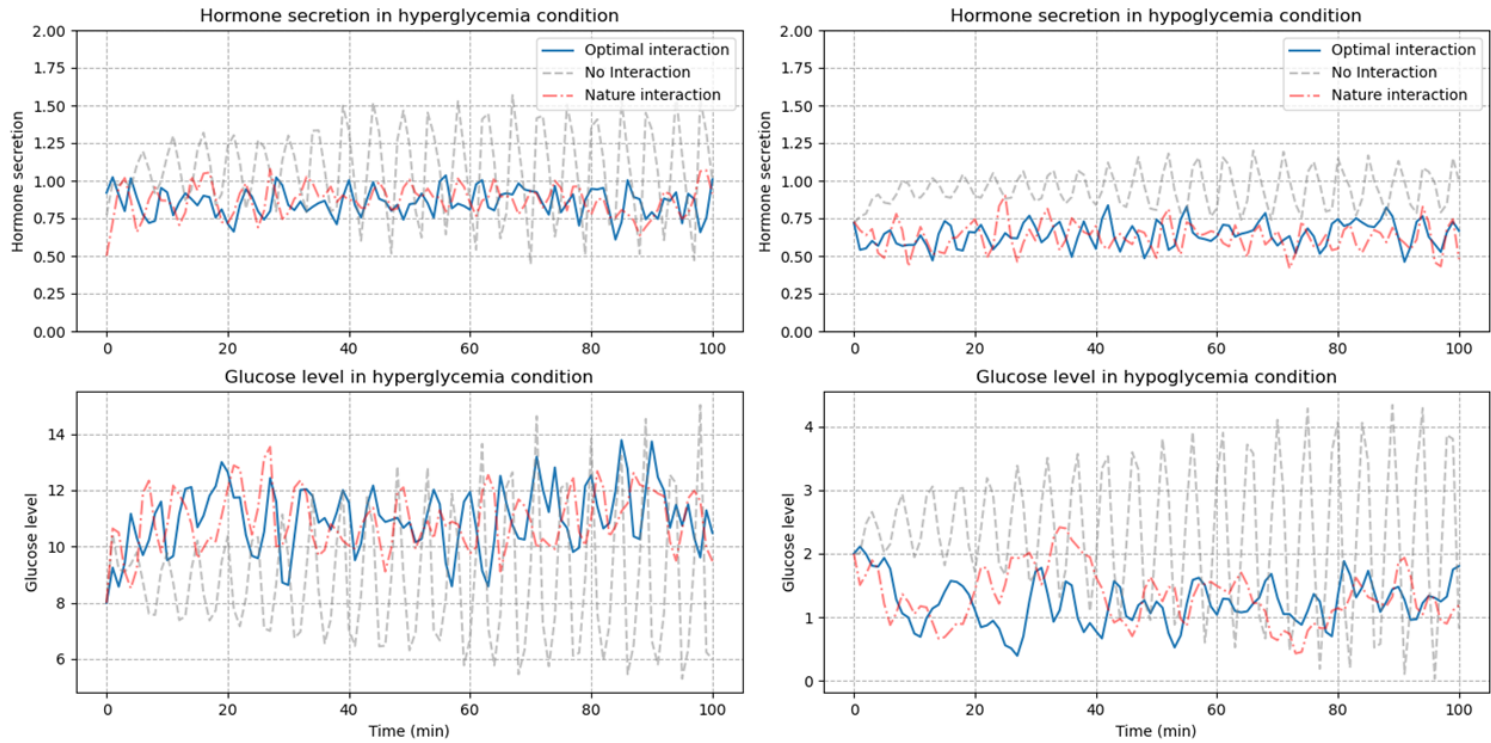


Figure 3.4: Temporal dynamics of hormone secretion and glucose levels by Interaction type in varied glucose conditions. For the high glucose condition, shown on the left, the figures demonstrate the response patterns in an elevated glucose environment. Conversely, the right side of the figure focuses on the low glucose condition.

### 3.3.2 The impact of the number of islets

Our investigation aimed to discern how the number of islets influences the optimal interaction for regulating blood glucose levels. To this end, we first analyzed the cumulative rewards, as defined by Equation (3.1), across various numbers of islets under normoglycemic conditions, both in scenarios without interactions and in those reflecting naturally observed interaction patterns. These analyses were systematically compiled in Table 3.1, revealing a trend where an increase in islet count corresponded to a rise in cumulative reward. Notably, the increment in reward plateaued for islet counts exceeding 50, suggesting a threshold beyond which additional islets do not significantly enhance reward.

Further, we visualized the impact of islet quantity on hormone secretion and glucose levels through Figures 3.5 and 3.6. These illustrations indicated that while the average hormone secretion and glucose levels remained consistent across different islet counts, an increase in islet quantity led to reduced fluctuations, thereby promoting stability. This observation aligns with the reward trends presented in Table 3.1, where an augmented number of islets contributes to enhanced system stability and efficiency.

To examine how optimal interactions, as identified through reinforcement learning, adapt to variations in the number of islets, we expanded our investigation to include up to 200 islets under normal glucose conditions. This detailed analysis is thoroughly documented in Appendix C. Although no single interaction pattern exclusively dominated the results, we observed a consistent trend where the emerging interactions predominantly fell into Type 1 or Type 2 categories. Notably, under both high and low glucose conditions, a specific interaction was recurrently observed, exhibiting a remarkable consistency in frequency regardless of the number of islets. This interaction, closely mirroring the pattern naturally observed within islets, highlights the intrinsic adaptability and efficacy of natural interaction mechanisms across diverse glucose levels and islet quantities.

The identification of this optimal interaction in scenarios with a substantial islet

count, as illustrated in Figure 3.7, underscores the findings. When compared to Figure 3.2, this observation affirms the persistence of naturally occurring interaction types, underlining their essential role in the regulatory functions of islets. Such consistency across different experimental setups emphasizes the significant impact of interaction type on hormone secretion and glucose level stability.

Islet Number ( $N$ )	Avg. Reward	
	No interaction	Nature interaction
1	-144.63	-75.56
5	-86.88	-63.46
20	-73.71	-46.17
50	-57.18	-42.01
200	-56.12	-37.79
500	-56.87	-35.35
1000	-54.50	-35.03

Table 3.1: Cumulative reward over 50 timesteps as a function of islet number in normoglycemic conditions without interactions.



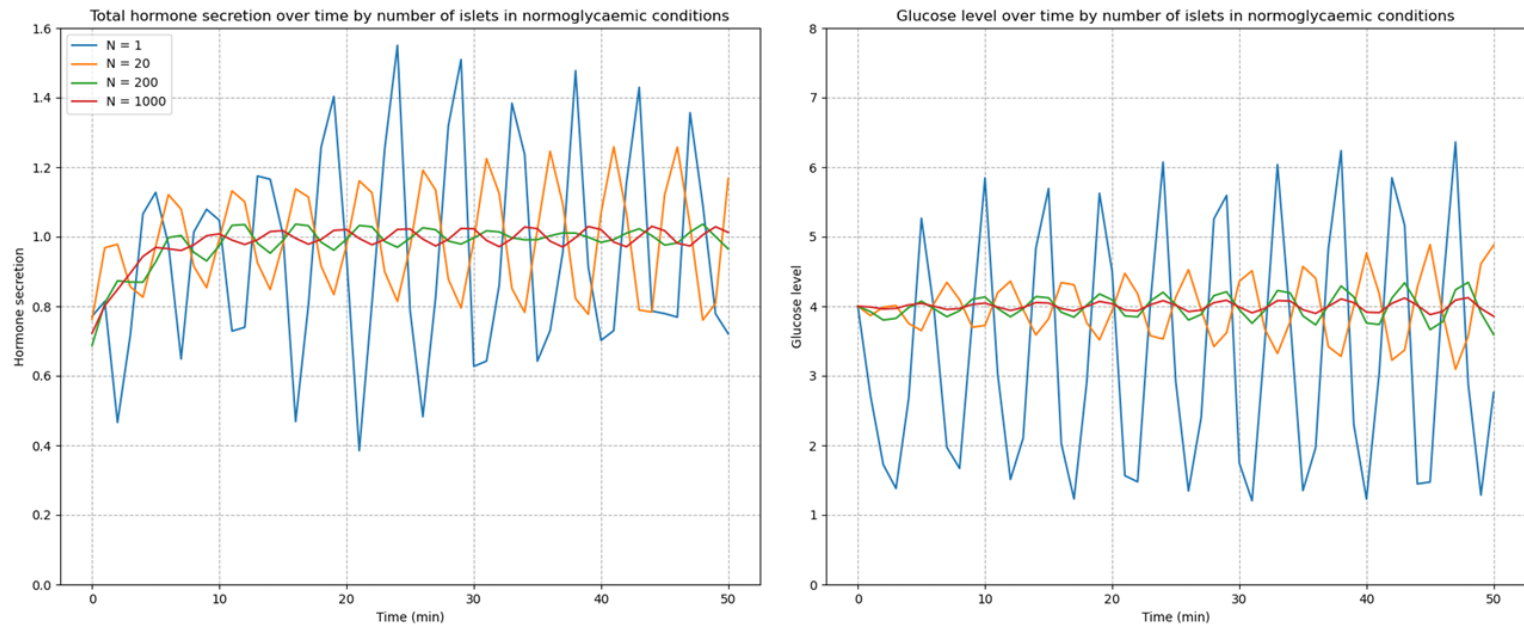


Figure 3.5: Hormone secretion and glucose level by islet number in the absence of interaction. Generally the higher the islet number, the more stable the hormone secretion and the glucose level.

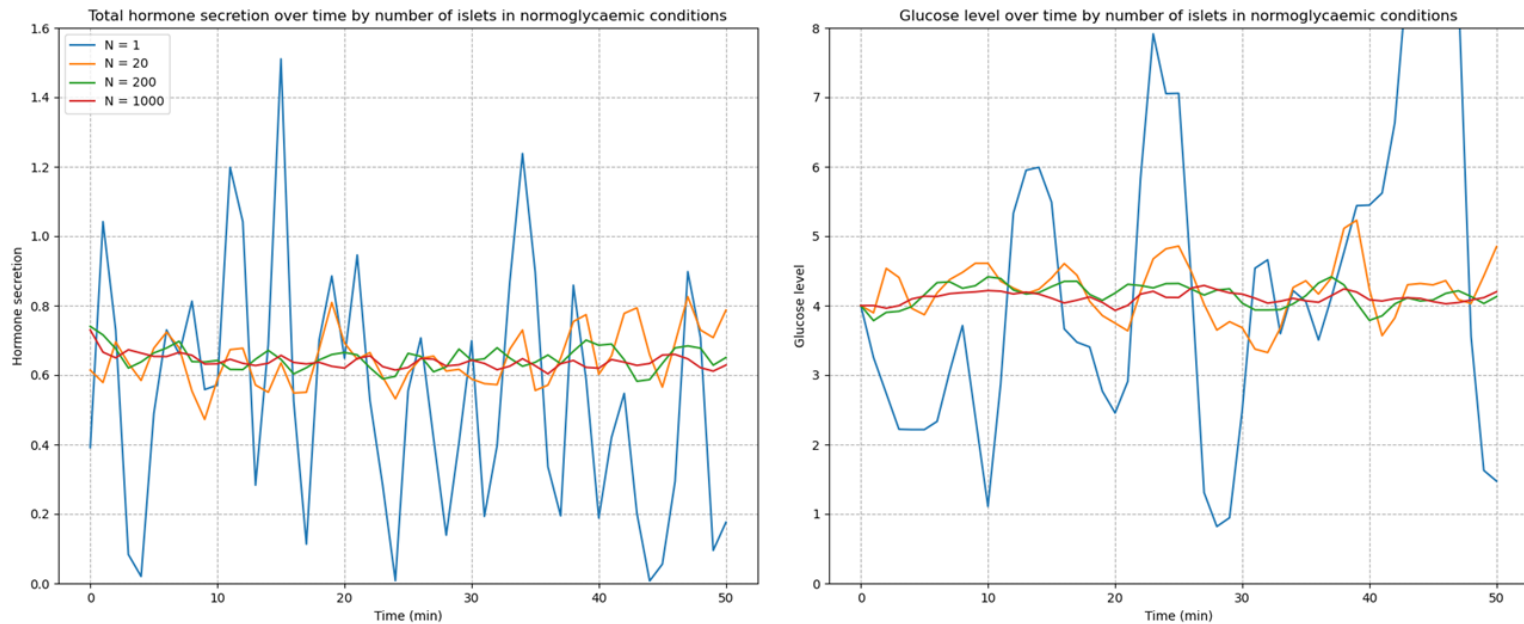


Figure 3.6: Hormone secretion and glucose level by islet number in the nature interaction, at high glucose. Generally the higher the islet number, the more stable the hormone secretion and the glucose level.

Top 5 most frequent interactions in hyperglycemia condition when the number of islet is 200					
Interaction					
Percentage (%)	25	18	13	10	9
Type	1	2	1	1	1

Top 5 most frequent interactions in hypoglycemia condition when the number of islet is 200					
Interaction					
Percentage (%)	39	15	6	6	5
Type	1	1	2	1	1

Figure 3.7: Optimal interactions and their percentages in high blood sugar (top) and low blood sugar (bottom) when the number of islets was 200. The natural interactions were first in high blood sugar and second in low blood sugar.

## Chapter 4

### Conclusion

This thesis leveraged the Multi-Agent Multi-Armed Bandit (MAMAB) framework within reinforcement learning to investigate the complex interactions of  $\alpha$ ,  $\beta$ , and  $\delta$  cells in the islets of Langerhans, aiming to elucidate the mechanisms that underpin efficient blood glucose homeostasis. Conducting experiments under a variety of glycemic conditions and with different numbers of Langerhans islets, we discovered that naturally occurring interaction patterns are particularly effective, especially in managing extreme hyperglycemic and hypoglycemic states.

The initial phase of our research indicated that interactions leading to mutual inhibition or promotion of hormone secretion between two cells were generally detrimental to maintaining glycemic equilibrium. In contrast, interaction patterns observed in nature proved to be highly beneficial in stabilizing blood glucose levels in both high and low glycemic scenarios, emphasizing the significance of natural cellular coordination.

Further exploration revealed that increasing the number of islets contributes to more stable blood glucose and hormone levels. However, it became evident that after reaching a certain number of islets, additional increases did not significantly enhance this stability. When we applied the MAMAB framework to identify optimal interactions, we found that while these interactions varied with the islet count under normoglycemic conditions, specific interaction patterns, akin to those observed in nature,

consistently emerged in hyperglycemic and hypoglycemic environments, regardless of islet quantity.

A critical aspect of this study was acknowledging the limitations of using reinforcement learning to mimic the evolutionary processes of biological organisms. RL models, including those based on the UCB algorithm as used in our study, simplify the vast complexities of genetic, metabolic, and environmental interactions that drive biological evolution. They do not account for genetic variation, phenotypic diversity, or the mechanisms of reproduction and natural selection, fundamental to evolutionary biology. Additionally, the relatively short timescale of RL models contrasts with the extensive temporal span of biological evolution, which occurs over many generations and vast epochs.

Our investigation sought to understand why natural interaction patterns are more advantageous for hormonal and glucose regulation compared to other similar interactions. We hypothesized that reinforcement learning, often paralleled with biological evolution, might offer insights into why islet cell interactions have evolved to mirror those observed in nature. Despite the limitations of RL in fully representing evolutionary processes, our findings provide a novel perspective that could illuminate the evolutionary rationale behind the specific cellular interactions prevalent in the islets of Langerhans.

In conclusion, this research not only deepens our understanding of the dynamics within the islets of Langerhans but also validates the potential of reinforcement learning in modeling such complex biological systems. Future research delving into the nature of these cellular interactions is expected to further advance our knowledge of endocrine physiology and underscore the applicability of reinforcement learning in biological studies.

# Bibliography

- [1] A. Paniccia and R. D. Schulick, “Pancreatic physiology and functional assessment,” in *Blumgart’s Surgery of the Liver, Biliary Tract and Pancreas, 2-Volume Set*, Elsevier, 2017, pp. 66–76.
- [2] D.-S. Koh, J.-H. Cho, and L. Chen, “Paracrine interactions within islets of langerhans,” *Journal of molecular neuroscience*, vol. 48, pp. 429–440, 2012.
- [3] A. A. Elayat, M. M. el Naggar, and M. Tahir, “An immunocytochemical and morphometric study of the rat pancreatic islets.,” *Journal of anatomy*, vol. 186, no. Pt 3, p. 629, 1995.
- [4] D.-H. Park, T. Song, D.-T. Hoang, J. Xu, and J. Jo, “A local counter-regulatory motif modulates the global phase of hormonal oscillations,” *Scientific Reports*, vol. 7, no. 1, p. 1602, 2017.
- [5] T. Song and J. Jo, “Tripartite cell networks for glucose homeostasis,” *Physical biology*, vol. 16, no. 5, p. 051 001, 2019.
- [6] D. E. Moriarty, A. C. Schultz, and J. J. Grefenstette, “Evolutionary algorithms for reinforcement learning,” *Journal of Artificial Intelligence Research*, vol. 11, pp. 241–276, 1999.
- [7] S. Khadka and K. Tumer, “Evolutionary reinforcement learning,” *arXiv preprint arXiv:1805.07917*, vol. 223, 2018.

- [8] D. E. Koulouriotis and A Xanthopoulos, “Reinforcement learning and evolutionary algorithms for non-stationary multi-armed bandit problems,” *Applied Mathematics and Computation*, vol. 196, no. 2, pp. 913–922, 2008.
- [9] G. Da Silva Xavier, “The cells of the islets of langerhans,” *Journal of clinical medicine*, vol. 7, no. 3, p. 54, 2018.
- [10] C. Ionescu-Tirgoviste, P. A. Gagniuc, E. Gubceac, *et al.*, “A 3d map of the islet routes throughout the healthy human pancreas,” *Scientific reports*, vol. 5, no. 1, p. 14 634, 2015.
- [11] M. Brissova, M. J. Fowler, W. E. Nicholson, *et al.*, “Assessment of human pancreatic islet architecture and composition by laser scanning confocal microscopy,” *Journal of Histochemistry & Cytochemistry*, vol. 53, no. 9, pp. 1087–1097, 2005.
- [12] O. Cabrera, D. M. Berman, N. S. Kenyon, C. Ricordi, P.-O. Berggren, and A. Caicedo, “The unique cytoarchitecture of human pancreatic islets has implications for islet cell function,” *Proceedings of the National Academy of Sciences*, vol. 103, no. 7, pp. 2334–2339, 2006.
- [13] R. S. Sutton and A. G. Barto, *Reinforcement learning: An introduction*. MIT press, 2018.
- [14] A. Slivkins *et al.*, “Introduction to multi-armed bandits,” *Foundations and Trends® in Machine Learning*, vol. 12, no. 1-2, pp. 1–286, 2019.
- [15] P. Auer, N. Cesa-Bianchi, and P. Fischer, “Finite-time analysis of the multi-armed bandit problem,” *Machine learning*, vol. 47, pp. 235–256, 2002.
- [16] K. Jamieson, M. Malloy, R. Nowak, and S. Bubeck, “Lil’ucb: An optimal exploration algorithm for multi-armed bandits,” in *Conference on Learning Theory*, PMLR, 2014, pp. 423–439.
- [17] D. Bouneffouf and R. Féraud, “Multi-armed bandit problem with known trend,” *Neurocomputing*, vol. 205, pp. 16–21, 2016.

- [18] J.-Y. Audibert, S. Bubeck, and R. Munos, “Best arm identification in multi-armed bandits,” in *COLT*, 2010, pp. 41–53.
- [19] V. Kuleshov and D. Precup, “Algorithms for multi-armed bandit problems,” *arXiv preprint arXiv:1402.6028*, 2014.
- [20] D. Vial, S. Shakkottai, and R. Srikant, “Robust multi-agent multi-armed bandits,” in *Proceedings of the Twenty-second International Symposium on Theory, Algorithmic Foundations, and Protocol Design for Mobile Networks and Mobile Computing*, 2021, pp. 161–170.
- [21] W. Chen, W. Hu, F. Li, J. Li, Y. Liu, and P. Lu, “Combinatorial multi-armed bandit with general reward functions,” *Advances in Neural Information Processing Systems*, vol. 29, 2016.
- [22] M. Agarwal, V. Aggarwal, and K. Azizzadenesheli, “Multi-agent multi-armed bandits with limited communication,” *The Journal of Machine Learning Research*, vol. 23, no. 1, pp. 9529–9552, 2022.
- [23] P. Auer and R. Ortner, “Ucb revisited: Improved regret bounds for the stochastic multi-armed bandit problem,” *Periodica Mathematica Hungarica*, vol. 61, no. 1-2, pp. 55–65, 2010.



# **Appendices**

## Appendix A

### Top Reward Table by Interaction Type

In Appendix A of our study, we undertake a comprehensive analysis of cellular interactions within an islet. Given that each cell type –  $\alpha$ ,  $\beta$ , and  $\delta$  – can engage in one of nine distinct actions, this results in a total of  $9^3 = 729$  unique interaction combinations. To evaluate the effectiveness of these interactions, we conducted a meticulous assessment of their rewards.

For each of the 729 interaction types, we calculated the average total reward. This was derived from conducting five separate trials, with each trial encompassing 100 timesteps. Such an approach ensures a robust evaluation by averaging out anomalies and focusing on consistent patterns across multiple iterations.

Post this meticulous computation, we collated the interactions yielding the highest rewards for each specific glucose condition tested in our experiments. These top-performing interactions, based on the average total reward, are tabulated in tables [A.1](#), [A.2](#), [A.3](#) and [A.4](#).

Avg. Reward	$\alpha \rightarrow \beta$	$\alpha \rightarrow \delta$	$\beta \rightarrow \alpha$	$\beta \rightarrow \delta$	$\delta \rightarrow \alpha$	$\delta \rightarrow \beta$	Type
-86.05	+1	-1	0	-1	+1	+1	1
-86.30	+1	+1	0	+1	-1	-1	1
-88.03	0	-1	+1	-1	+1	+1	1
-88.49	0	+1	+1	+1	-1	-1	1
-89.19	-1	+1	+1	+1	-1	-1	1

Table A.1: Top reward table in normal glucose settings

Avg. Reward	$\alpha \rightarrow \beta$	$\alpha \rightarrow \delta$	$\beta \rightarrow \alpha$	$\beta \rightarrow \delta$	$\delta \rightarrow \alpha$	$\delta \rightarrow \beta$	Type
-874.50	+1	+1	-1	+1	-1	-1	1
-883.89	+1	+1	-1	+1	0	-1	1
-884.98	-1	+1	+1	-1	-1	+1	2
-887.23	-1	+1	+1	-1	0	+1	2
-889.04	+1	0	0	0	-1	-1	1

Table A.2: Top reward table in high glucose settings

Avg. Reward	$\alpha \rightarrow \beta$	$\alpha \rightarrow \delta$	$\beta \rightarrow \alpha$	$\beta \rightarrow \delta$	$\delta \rightarrow \alpha$	$\delta \rightarrow \beta$	Type
-198.03	-1	-1	+1	0	+1	0	1
-202.86	+1	+1	-1	0	-1	-1	1
-203.06	+1	+1	-1	-1	-1	0	1
-203.26	+1	-1	-1	+1	+1	-1	2
-204.01	-1	+1	+1	-1	-1	+1	2

Table A.3: Top reward table in low glucose settings

Avg. Reward	$\alpha \rightarrow \beta$	$\alpha \rightarrow \delta$	$\beta \rightarrow \alpha$	$\beta \rightarrow \delta$	$\delta \rightarrow \alpha$	$\delta \rightarrow \beta$	Type
-206.20	-1	-1	+1	-1	+1	+1	1
-215.91	-1	-1	+1	0	+1	0	1
-218.65	+1	-1	-1	+1	+1	-1	2
-219.77	+1	+1	-1	+1	-1	-1	1
-219.96	-1	0	+1	-1	0	+1	1

Table A.4: Top reward table in non-stationary glucose settings

## Appendix B

### Optimal Interactions Relative to the Reward Coefficient

The parameter  $\rho$  in our study plays a pivotal role in determining the relative significance of hormone secretion versus glucose fluctuations within the reward structure. When  $\rho$  is set higher, it steers the agent towards prioritizing the minimization of hormone secretion. Conversely, a lower  $\rho$  value shifts the agent’s focus towards stabilizing glucose levels. For our experiments, we opted for  $\rho = 1$  in the normoglycemic state to equally weigh both the hormone secretion and glucose fluctuation components of the reward, considering their comparable magnitudes in this context.

To explore how variations in  $\rho$  influence the interactions, we conducted experiments with different  $\rho$  values, thereby altering the coefficient of importance. The outcomes of these experiments, showcasing how the interaction patterns shift with varying  $\rho$ , are systematically compiled and presented in a tabular format. This approach allows us to comprehensively understand the impact of altering the reward’s emphasis between hormone secretion and glucose fluctuation on the behavior of the agents.

Percentage (%)	$\alpha \rightarrow \beta$	$\alpha \rightarrow \delta$	$\beta \rightarrow \alpha$	$\beta \rightarrow \delta$	$\delta \rightarrow \alpha$	$\delta \rightarrow \beta$	Type
15	-1	-1	+1	-1	+1	+1	1
10	-1	-1	+1	0	+1	0	1
10	+1	-1	-1	+1	+1	-1	2
9	+1	+1	-1	+1	-1	-1	1
8	-1	0	+1	-1	0	+1	1

Table B.1: Top-5 frequent interaction table at  $\rho = 2$  in stationary glucose settings

Percentage (%)	$\alpha \rightarrow \beta$	$\alpha \rightarrow \delta$	$\beta \rightarrow \alpha$	$\beta \rightarrow \delta$	$\delta \rightarrow \alpha$	$\delta \rightarrow \beta$	Type
11	+1	+1	-1	+1	-1	-1	1
11	-1	-1	+1	-1	+1	+1	1
8	-1	+1	+1	+1	-1	-1	1
7	+1	-1	-1	0	+1	0	2
6	-1	+1	+1	-1	-1	+1	2

Table B.2: Top-5 frequent interaction table at  $\rho = 5$  in stationary glucose settings

Percentage (%)	$\alpha \rightarrow \beta$	$\alpha \rightarrow \delta$	$\beta \rightarrow \alpha$	$\beta \rightarrow \delta$	$\delta \rightarrow \alpha$	$\delta \rightarrow \beta$	Type
11	+1	+1	-1	-1	-1	+1	1
10	+1	-1	-1	+1	+1	-1	2
9	+1	-1	-1	0	+1	0	1
8	-1	-1	+1	-1	+1	+1	1
6	-1	+1	+1	-1	-1	+1	2

Table B.3: Top-5 frequent interaction table at  $\rho = 10$  in stationary glucose settings

Percentage (%)	$\alpha \rightarrow \beta$	$\alpha \rightarrow \delta$	$\beta \rightarrow \alpha$	$\beta \rightarrow \delta$	$\delta \rightarrow \alpha$	$\delta \rightarrow \beta$	Type
17	+1	+1	0	0	-1	-1	1
16	+1	+1	0	+1	-1	-1	1
14	0	+1	+1	+1	-1	-1	1
13	+1	-1	0	-1	+1	+1	1
12	0	-1	+1	-1	+1	+1	1

Table B.4: Top-5 frequent interaction table at  $\rho = 0.5$  in stationary glucose settings

Percentage (%)	$\alpha \rightarrow \beta$	$\alpha \rightarrow \delta$	$\beta \rightarrow \alpha$	$\beta \rightarrow \delta$	$\delta \rightarrow \alpha$	$\delta \rightarrow \beta$	Type
11	+1	0	0	+1	0	-1	1 & 2
10	+1	+1	0	0	-1	-1	1
9	+1	0	0	-1	0	+1	1
8	0	-1	+1	0	+1	0	1
7	0	+1	+1	0	-1	0	1 & 2

Table B.5: Top-5 frequent interaction table at  $\rho = 0.2$  in stationary glucose settings

Percentage (%)	$\alpha \rightarrow \beta$	$\alpha \rightarrow \delta$	$\beta \rightarrow \alpha$	$\beta \rightarrow \delta$	$\delta \rightarrow \alpha$	$\delta \rightarrow \beta$	Type
15	+1	0	0	+1	0	-1	1 & 2
7	+1	0	0	-1	0	+1	1
6	+1	+1	+1	+1	-1	-1	etc.
6	0	-1	+1	0	+1	0	1
6	0	+1	+1	0	-1	0	1 & 2

Table B.6: Top-5 frequent interaction table at  $\rho = 0.1$  in stationary glucose settings

## Appendix C

### Experimental results of optimal interaction based on the number of islets

Percentage (%)	$\alpha \rightarrow \beta$	$\alpha \rightarrow \delta$	$\beta \rightarrow \alpha$	$\beta \rightarrow \delta$	$\delta \rightarrow \alpha$	$\delta \rightarrow \beta$	Type
7	+1	-1	0	+1	0	0	1
7	0	-1	+1	0	+1	0	1
7	+1	-1	0	0	+1	+1	1
6	+1	+1	0	-1	0	0	1
5	+1	0	0	-1	0	+1	1

Table C.1: Top-5 optimal interactions at islet number  $N = 1$

Percentage (%)	$\alpha \rightarrow \beta$	$\alpha \rightarrow \delta$	$\beta \rightarrow \alpha$	$\beta \rightarrow \delta$	$\delta \rightarrow \alpha$	$\delta \rightarrow \beta$	Type
22	+1	-1	0	+1	0	0	1
14	0	-1	+1	0	+1	0	1
13	+1	-1	0	0	+1	+1	1
11	+1	+1	0	-1	0	0	1
9	+1	0	0	-1	0	+1	1

Table C.2: Top-5 optimal interactions at islet number  $N = 5$

Percentage (%)	$\alpha \rightarrow \beta$	$\alpha \rightarrow \delta$	$\beta \rightarrow \alpha$	$\beta \rightarrow \delta$	$\delta \rightarrow \alpha$	$\delta \rightarrow \beta$	Type
17	0	-1	+1	-1	+1	+1	1
16	0	+1	+1	+1	-1	-1	1
14	+1	+1	0	+1	-1	-1	1
13	+1	-1	0	0	+1	+1	1
11	+1	-1	0	-1	+1	+1	1

Table C.3: Top-5 optimal interactions at islet number  $N = 10$

Percentage (%)	$\alpha \rightarrow \beta$	$\alpha \rightarrow \delta$	$\beta \rightarrow \alpha$	$\beta \rightarrow \delta$	$\delta \rightarrow \alpha$	$\delta \rightarrow \beta$	Type
14	-1	-1	+1	-1	+1	+1	1
10	+1	+1	0	+1	-1	-1	1
10	+1	-1	0	-1	+1	+1	1
9	+1	-1	-1	+1	+1	-1	2
7	-1	+1	+1	+1	-1	-1	1

Table C.4: Top-5 optimal interactions at islet number  $N = 50$

Percentage (%)	$\alpha \rightarrow \beta$	$\alpha \rightarrow \delta$	$\beta \rightarrow \alpha$	$\beta \rightarrow \delta$	$\delta \rightarrow \alpha$	$\delta \rightarrow \beta$	Type
12	-1	+1	+1	+1	-1	-1	1
12	-1	-1	+1	-1	+1	+1	1
10	-1	-1	+1	0	+1	0	1
9	+1	+1	-1	+1	-1	-1	1
8	+1	+1	0	+1	-1	-1	1

Table C.5: Top-5 optimal interactions at islet number  $N = 100$

Percentage (%)	$\alpha \rightarrow \beta$	$\alpha \rightarrow \delta$	$\beta \rightarrow \alpha$	$\beta \rightarrow \delta$	$\delta \rightarrow \alpha$	$\delta \rightarrow \beta$	Type
10	+1	-1	-1	+1	+1	-1	2
9	+1	+1	-1	+1	-1	-1	1
8	+1	-1	-1	-1	+1	+1	1
8	-1	-1	+1	+1	+1	-1	1
7	-1	+1	+1	+1	-1	-1	1

Table C.6: Top-5 optimal interactions at islet number  $N = 200$



# 초 록

알파, 베타, 델타 세포로 구성된 랑게르한스 섬은 호르몬 조절을 통해 체내 혈당 항상성 유지에 있어 핵심적인 역할을 수행한다. 본 연구는 이전 연구를 바탕으로 구성된 환경 내에서 강화학습을 활용해 이들 세포의 조절 메커니즘을 분석하는 새로운 접근법을 제시한다. 우리는 다중 에이전트 다중 선택 문제(MAMAB)로서 문제를 정의하고, 세포 간 최적의 상호작용을 탐구하기 위해 상위 신뢰 경계(UCB) 방법을 적용했다.

실험은 두 가지 단계로 구성된다. 첫째, 강화학습을 통해 다양한 혈당 조건 하에서 최적의 세포 간 상호작용을 분석했다. 둘째, 섬의 수가 이러한 상호작용 및 시스템 전반의 안정성에 어떠한 영향을 미치는지 분석했다. 실험 결과, 특정 상호작용들이 섬의 수와 무관하게 고혈당 및 저혈당 상황에서도 혈당 항상성을 유지하고 혈당 변화에 효과적으로 대응하는 것으로 나타났다.

본 연구는 호르몬 분비량과 혈당 변동 값을 이용해 하나의 수치적 평가 체계로 통합함으로써 세포 상호작용의 평가에 있어 새로운 방법을 제시했다. 또한, 다양한 조건에서 강화학습을 통해 랑게르한스 섬 내 효과적인 세포 간 상호작용의 종류를 밝혀내고, 이로서 강화학습이 섬 세포 상호작용을 분석하는데 있어 진화적 및 기능적인 통찰을 제공할 수 있음을 보인다.

**주요어:** 혈당 항상성, 랑게르한스 섬, 강화학습, 멀티 에이전트 멀티 암드 밴딧, 세포 간 상호작용

**학번:** 2022-25506